

A metabolic database for biomedical studies of biopsy specimens by high-resolution magic angle spinning nuclear MR: A qualitative and quantitative tool

Elisa Ruhland^{1,2} | Caroline Bund^{1,2,3} | Hassiba Outilaft^{1,3} | Martial Piotto⁴ | Izzie-Jacques Namer^{1,2,3}

¹MNMS Platform, Hôpitaux Universitaires de Strasbourg, Strasbourg, France

²Service de Biophysique et Médecine Nucléaire, Hôpitaux Universitaires de Strasbourg, Strasbourg, France

³ICube, Université de Strasbourg / CNRS (UMR 7357), Strasbourg, France

⁴Bruker BioSpin, Wissembourg, France

Correspondence

Izzie-Jacques Namer, Service de Biophysique et de Médecine Nucléaire, Hôpitaux Universitaires de Strasbourg, Hôpital de Hautepierre, 1, avenue Mollière, 67098 Strasbourg Cedex 09, France.
Email: izzie.jacques.namer@chru-strasbourg.fr
Twitter: @mnmsPlatform

Purpose: The aim of this study is to generate a metabolic database for biomedical studies of biopsy specimens by high-resolution magic angle spinning (HRMAS) nuclear MR (NMR).

Methods: Seventy-six metabolites, classically found in human biopsy samples, were prepared in aqueous solution at a known concentration and analyzed by HRMAS NMR. The spectra were recorded under the same conditions as the ones used for the analysis of biopsy specimens routinely performed in our hospital.

Results: For each metabolite, a complete set of NMR spectra (1D ¹H, 1D ¹H-CPMG, 2D J-Resolved, 2D TOCSY, and 2D ¹H-¹³C HSQC) was recorded at 500 MHz and 277 K. All spectra were manually assigned using the information contained in the different spectra and existing databases. Experiments to measure the T₁ and the T₂ of the different protons present in the 76 metabolites were also recorded.

Conclusion: This new HRMAS metabolic database is a useful tool for all scientists working on human biopsy specimens, particularly in the field of oncology. It will make the identification of metabolites in biopsy specimens faster and more reliable. Additionally, the knowledge of the T₁ and T₂ values will allow to obtain a more accurate quantification of the metabolites present in biopsy specimens.

KEY WORDS

biopsies, database, HRMAS NMR, metabolomics

1 | INTRODUCTION

Metabolomics is a technique that has developed considerably over the past few years. It provides a link between the

genotype and metabolic phenotype and allows a better understanding of cellular metabolism by revealing the metabolite concentration impacted by down- or upregulation of a specific gene transcript in pathological conditions.¹ Metabolomics

This is an open access article under the terms of the Creative Commons Attribution-NonCommercial-NoDerivs License, which permits use and distribution in any medium, provided the original work is properly cited, the use is non-commercial and no modifications or adaptations are made.

© 2019 The Authors. *Magnetic Resonance in Medicine* published by Wiley Periodicals, Inc. on behalf of International Society for Magnetic Resonance in Medicine

is particularly useful to characterize the biology of the tumor, monitor treatments, and predict toxicity.² Nuclear MR (NMR) metabolomics of tissues has been used to study several cancers³ and has the potential to enable personalized treatment.

High-resolution magic angle spinning (HRMAS) NMR spectroscopy is particularly adapted to study small samples of unprocessed tissue specimens for medical indications such as tumor analysis⁴ and transplantation.⁵ The preparation of biopsy samples is straightforward and fast,⁶ obviating the need for lengthy chemical extraction procedures. HRMAS NMR spectroscopy can identify and quantify several metabolites from 1D ¹H NMR spectra with excellent resolution and signal-to-noise ratio. In clinical routine, this technique could eventually be used to characterize biopsies and find predictive and prognostic factors during surgery. In our hospital, samples are transported rapidly by a pneumatic tube from the operating room to the room where the NMR spectrometer is located. Acquisition of HRMAS data takes only around 20 minutes.^{4,6-8}

HRMAS NMR has the potential to provide important medical benefits; however, metabolite identification and quantification needs to be fast and reliable. Identification is usually based on the literature and existing databases that have been developed mainly for urine, plasma and CSF⁹ (HMDB: <http://www.hmdb.ca/>).^{10,11} A specific HRMAS database for the study of human biological tissues is still lacking and needs to be developed. Moreover, quantification is essential for network analysis and discovery of new biomarkers. The aim of this study is to generate a metabolic HRMAS database for the 76 most common metabolites found in human tissues.

2 | METHODS

2.1 | Preparation of metabolite solutions

2.1.1 | Pure metabolite standards

A total of 76 metabolite solutions were prepared to build the metabolic database. For each metabolite, a solution containing approximately 3 mM of the pure metabolite was prepared in D₂O containing 9.4 mM of phosphate-buffered saline (PBS) buffer (pH 7.4) and 0.125% trisodium phosphate (TSP). Twenty-four microliters of this solution were placed in a 25-µL disposable insert in KeLF. The number of nmoles actually present in the inserts of each standard solution was determined exactly using the Eretic¹² method (Table 1).

2.1.2 | Standard metabolites mixture for the validation of concentration measurements

Four solutions containing 4 metabolites were prepared in the same D₂O/PBS buffer at different concentrations to validate

concentration measurements, taking into account T₁ and T₂ effects.

The content of the 4 solutions is listed below:

- Mixture 1: acetate, ascorbate, choline, and hypotaurine (19.68, 19.44, 19.92, and 20.4 nmoles, respectively);
- Mixture 2: acetate, ascorbate, choline, and hypotaurine (32.16, 31.92, 32.64, and 33.36 nmoles, respectively);
- Mixture 3: acetate ascorbate, choline and hypotaurine (41.04, 40.8, 41.52, and 42.48 nmoles, respectively); and
- Mixture 4: acetate, ascorbate, choline, and hypotaurine (53.52, 53.28, 54.24, and 53.04 nmoles, respectively).

2.1.3 | Biopsies preparation

The protocol is the one classically used in our laboratory to prepare biopsy specimens: All tissue samples were collected during surgery immediately after removal of the tumor. Specimens were either frozen in liquid nitrogen in an appropriate Dewar in the operating room or transferred from the block to the spectrometer room by a pneumatic system. Samples were then prepared at a temperature of -20°C. Amount of tissue used ranged from 15 to 20 mg. Each tissue sample was placed in a 25 µL disposable insert using a biopsy punch. A volume of 10 µL of deuterium oxide was then added to each biopsy insert. After a centrifugation step, deuterium oxide was added again to fill the insert. Finally, inserts were stored at -80°C. until the HRMAS analysis was performed. The insert was then placed in a 4-mm ZrO₂ rotor and inserted into the NMR spectrometer. All assays were performed at 4°C. After the analysis, inserts were stored back at -80°C.

2.2 | HRMAS NMR spectroscopic analysis

All experiments were conducted on a Bruker Avance III 500 MHz NMR spectrometer (Bruker BioSpin, Billerica, MA) installed at Strasbourg University Hospitals (www.mnms-platform.com). The spectrometer is equipped with a triple-resonance (¹H, ¹³C, and ³¹P) HRMAS probe. The temperature was set to 277 K for all acquisitions. Spinning speed was set to 3502 Hz in order to keep the rotation sidebands out of the spectrum window and to minimize sample degradation. For each standard metabolite solution, a complete set of NMR experiments was recorded under exactly the same experimental conditions as the ones used in our laboratory when analyzing human tissues.^{6,8} A 1-dimensional ¹H CPMG spectrum was first recorded and followed by a 1-pulse^{5,6} experiment in order to check the stability of the metabolites. For all metabolites, the following 2D experiments were then recorded: J-Resolved,¹³ TOCSY,^{14,15}

TABLE 1 Content of the metabolic database

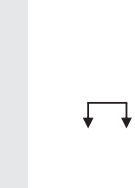
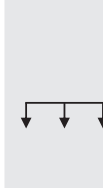
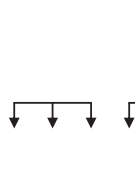
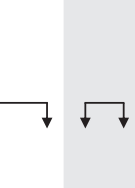
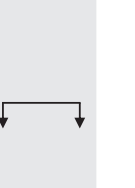
Metabolite (nanomoles)	Group	Structure	T ₁ (s)	T ₂ (s)	T ₁ /T ₂	Loss with J (Hz)	*δ ¹ H (ppm)	ppm range	TOCSY coupling	*δ ¹³ C (ppm)
(a) Compounds without ³¹ P										
2-hydroxyglutarate (39.59 nmoles)	• ¹ CH ₂		0.671	0.474	0.181	m	1.84	[1.90...1.79]	↓	33.81
	¹ CH ₂		0.638	0.527	0.164	m	1.99	[2.04...1.95]	↓	33.50
	² CH ₂		0.699	0.583	0.150	m	2.26	[2.34...2.18]	↓	36.15
	³ CH		1.47	0.755	0.160	dd (4.0Hz; 7.8Hz)	4.03	[4.06...4.01]	↓	74.71
2-ketoglutarate (64.51 nmoles)	• ¹ CH ₂		1.21	0.689	0.169	t (6.7Hz)	2.45	[2.47...2.42]	↓	33.08
	² CH ₂		1.41	0.589	0.165	t (6.7Hz)	3.01	[3.04...3.00]	↓	38.25
3-hydroxybutyrate (52.64 nmoles)	• ¹ CH ₃		0.78	0.510	0.171	d (6.3Hz)	1.20	[1.22...1.18]	↓	24.35
	² CH ₂		1.02	0.804	0.122	dd (6.7Hz; 14.2Hz)	2.30	[2.33...2.27]	↓	49.13
	² CH ₂		1.02	0.828	0.119	dd (6.7Hz; 14.2Hz)	2.42	[2.46...3.39]	↓	49.28
	³ CH		1.98	0.632	0.171	dd (6.3Hz; 6.7Hz)	4.16	[4.20...4.12]	↓	68.31
5-HT (5-hydroxy-tryptophane) (36.52 nmoles)	• ¹ CH ₂		0.403	0.332	0.258	dd (8.3Hz; 15.3Hz)	3.24	[3.28...3.20]	↓	28.78
	¹ CH ₂		0.406	0.314	0.246	dd (4.8Hz; 15.4Hz)	3.41	[3.45...3.38]	↓	28.68
	² CH		1.24	0.790	0.133	dd (4.8Hz; 8.3Hz)	4.03	[4.06...4.00]	↓	57.024
	³ CH		2.00	1.43	0.165	dd (2.4Hz; 8.8Hz)	6.86	[6.88...6.84]	↓	114.16
	• ⁴ CH		2.08	1.72	0.164	d (2.4Hz)	7.14	[7.16...7.13]	↓	104.91
	⁵ CH		2.62	2.15	0.219	s	7.28	[7.29...7.26]	↓	128.17
	⁶ CH		2.01	1.47	0.165	d (8.8Hz)	7.41	[7.43...7.39]	↓	115.06
Acetate (71.1 nmoles)	• ¹ CH ₃		3.2	2.61	0.277	s	1.92	[1.93...1.91]	↓	25.9
Acetone (38.78 nmoles)	• ¹ CH ₃		5.78	5.13	0.473	s	2.23	[2.24...2.22]	32.82	
Adenosine (48.48 nmoles)	¹ CH ₂		0.52	0.313	0.259	dd (3.2Hz; 13Hz)	3.84	[3.87...3.82]	↓	64.09
	¹ CH ₂		0.491	0.302	0.267	dd (2.7Hz; 13Hz)	3.91	[3.95...3.89]	↓	64.09
	² CH		0.856	0.720	0.127	m	4.31	[4.32...4.29]	↓	88.54
	³ CH		1.15	0.701	0.144	dd (3.2Hz; 5.0Hz)	4.44	[4.46...4.42]	↓	73.29
	⁴ CH		1.04	0.701		dd (5.0Hz; 6.3Hz)	4.82	[4.84...4.79]	↓	76.23
	⁵ CH		1.53	1.16	0.128	d (6.3Hz)	6.07	[6.10...6.05]	↓	90.85
	⁶ CH		3.66	1.570	0.338	s	8.23	[8.24...8.22]	↓	143.1
	⁷ CH		1.77	1.14	0.154	s	8.34	[8.35...8.34]	↓	

(Continues)

TABLE 1 (Continued)

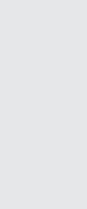
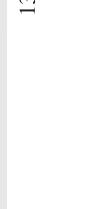
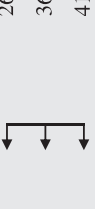
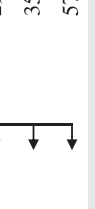
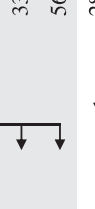
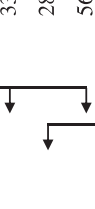
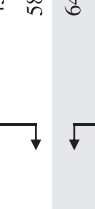
Metabolite (nanmoles)	Group	Structure	T ₁ (s)	T ₂ (s)	T ₁ /T ₂	Loss with	*δ ¹ H (ppm)	ppm range	TOCSY coupling	*δ ¹³ C (ppm)
Alanine (59.02 nmoles)	• ¹ CH ₃		1.05	0.832	0.12	d (7.2Hz)	1.48	[1.50...1.45]	↔	18.70
	² CH		3.12	1.12	0.302	q (7.2Hz)	3.78	[3.81...3.76]	↔	53.05
Allocystathione (34.06 nmoles)	¹ CH ₂		0.450	0.314	0.258	m	2.18	[2.25...2.11]	↔	32.52
	² CH ₂		0.456	0.373	0.222	m	2.72	[2.77...2.67]	↔	29.37
	• ³ CH ₂		0.440	0.340	0.241	dd (7.2Hz; 14.8Hz)	3.08	[3.12...3.05]	↔	34.31
	³ CH ₂		0.463	0.349	0.236	dd (4.4Hz; 14.8Hz)	3.15	[3.18...3.12]	↔	34.31
	⁴ CH		1.16	0.932	0.115	dd (5.5Hz; 7Hz)	3.87	[3.90...3.85]	↔	56.17
	⁵ CH		1.21	0.717	0.145	dd (4.4Hz; 7Hz)	3.96	[3.99...3.94]	↔	55.96
Anserine (53.15 nmoles)	¹ CH ₂		0.661	0.509	0.169	m	2.69	[2.78...2.61]	↔	34.58
	² CH ₂		0.413	0.275	0.289	dd (9.1Hz; 15.7Hz)	3.04	[3.09...3.00]	↔	28.43
	³ CH ₂					m	3.21	[3.27...3.16]	↔	28.43
	⁴ CH ₃		0.926	0.652	0.141	s	3.77	[3.81...3.75]	↔	38.14
	⁵ CH		1.15	0.769	0.133	dd (5.4Hz; 9.3Hz)	4.49	[4.54...4.46]	↔	34.91
	⁶ CH		1.58	0.712	0.176	s	7.07	[7.11...7.04]	↔	55.94
	• ⁷ CH		1.61	0.428	0.248	s	8.19	[8.23...8.17]	↔	123.56
Arginine (45.76 nmoles)	• ¹ CH ₂		0.485	0.325	0.251	m	1.64	[1.69...1.59]	↔	26.28
	¹ CH ₂		0.485	0.344	0.239	m	1.72	[1.79...1.69]	↔	30.17
	² CH ₂		0.477	0.473	0.180	m	1.92	[1.97...1.88]	↔	43.11
	³ CH ₂		0.523	0.369	0.224	t (6.8Hz)	3.25	[3.28...3.22]	↔	57.02
	⁴ CH		1.17	0.647	0.154	t (6.5Hz)	3.78	[3.80...3.75]	↔	65.12
Ascorbate (25.72 nmoles)	¹ CH ₂		0.616	0.519	0.166	m	3.74	[3.80...3.69]	↔	72.13
	² CH		1.50	0.98	0.143	m	4.02	[4.05...3.99]	↔	80.98
	• ³ CH		1.78	1.47	0.139	d (1.9Hz)	4.52	[4.55...4.51]	↔	36.95
Asparagine (47.97 nmoles)	¹ CH ₂		0.941	0.709	0.132	dd (7.5Hz; 17Hz)	2.87	[2.91...2.85]	↔	37.04
	• ¹ CH ₂		0.939	0.782	0.121	dd (4.3Hz; 17Hz)	2.95	[2.98...2.92]	↔	53.68
	² CH		2.99	1.53	0.273	dd (4.3Hz; 7.5Hz)	4.00	[4.03...4.99]	↔	38.93
Aspartate (42.28 nmoles)	¹ CH ₂		0.811	0.793	0.115	dd (8.7Hz; 17.5Hz)	2.69	[3.82...3.75]	↔	39.1
	• ¹ CH ₂		0.804	0.780	0.117	dd (3.8Hz; 17.5Hz)	2.81	[2.85...2.78]	↔	54.66
	² CH		2.24	1.71	0.184	dd (3.8Hz; 8.7Hz)	3.89	[2.73...2.65]	↔	(Continues)

TABLE 1 (Continued)

Metabolite (nanmoles)	Group	Structure	T ₁ (s)	T ₂ (s)	T ₁ /T ₂	Loss with J (Hz)	*δ ¹ H (ppm)	ppm range	TOCSY coupling	*δ ¹³ C (ppm)
Betaine (48.15 nmoles)	• ¹ CH ₃ ² CH ₂		1.3 1.71	0.788 1.5	0.141 0.131	s s	3.28 3.93	[3.31...3.24] [3.95...3.90]	56.06 68.67	
Choline (50.7 nmoles)	• ¹ CH ₃ ² CH ₂ ³ CH ₂		1.45 1.75 1.91	1.15 1.59 1.75	0.105 0.132 0.145	s m m	3.22 3.54 4.07	[3.24...3.20] [3.57...3.51] [4.10...3.04]	56.42 69.91 58.19	
Citrate (51.56 nmoles)	• ¹ CH ₂ ² CH ₂		0.480 0.482	0.389 0.397	0.214 0.210	d (15.3Hz) d (15.2Hz)	2.52 2.66	[2.55...2.50] [2.69...2.63]	47.99 47.99	
Creatine (52.39 nmoles)	• ¹ CH ₃ ² CH ₂		1.49 0.799	1.22 0.693	0.121 0.130	s s	3.03 3.94	[3.06...3.02] [3.96...3.92]	39.56 56.46	
Cysteine (181.81 nmoles)	¹ CH ₂ • ¹ CH ₂ ² CH		1.10 1.06 3.08	0.667 0.672 1.3	0.147 0.143 0.290	dd (4.0Hz; 15Hz) dd (5.6Hz; 15Hz) dd (4.0Hz; 5.6Hz)	3.01 3.09 3.98	[3.05...2.99] [3.13...3.07] [4.00...3.97]	27.42 27.42 58.36	
DOPA (3,4-dihydroxy-L-phenylalanine) (165.74 nmoles)	¹ CH ₂ ² CH ³ CH ⁴ CH ⁵ CH		0.377 0.348 1.10 1.26 1.73 1.71	0.318 0.260 0.747 0.946 1.54 1.25	0.255 0.303 0.134 0.121 0.132 0.142	dd (7.7Hz; 14.7Hz) dd (5.0Hz; 14.7Hz) dd (5.0Hz; 7.7Hz) dd (2.1Hz; 8.1Hz) d (2.1Hz) d (8.1Hz)	3.00 3.15 3.93 6.73 6.83 6.89	[3.04...2.97] [3.19...3.12] [3.96...3.90] [6.75...6.71] [6.84...6.81] [6.91...6.88]	38.17 38.17 58.49 124.35 119.4 119.02	
Dopamine (59.45 nmoles)	¹ CH ₂ ² CH ₂ • ³ CH ⁴ CH ⁵ CH		0.55 0.571 1.54 2.12 2.14	0.466 0.483 1.18 1.79 1.58	0.183 0.177 0.128 0.168 0.176	t (7.2Hz) t (7.2Hz) dd (2.1Hz; 8.1Hz) d (2.1Hz) d (8.1Hz)	2.88 3.22 6.76 6.86 6.90	[2.91...2.84] [3.25...3.19] [6.78...6.74] [6.87...6.84] [6.92...6.88]	34.7 43.11 123.68 119.15 118.99	
Epinephrine (81.86 nmoles)	¹ CH ₃ ² CH ₂ ³ CH ⁴ CH ⁵ CH ⁶ CH		0.830 0.443 1.44 1.90 1.84	0.572 0.300 0.864 0.663 1.11	0.155 0.268 0.144 0.216 0.164	s m dd (1.7Hz; 8.3Hz) d (8.1Hz) d (1.9Hz)	2.76 3.28 6.86 6.94 6.96	[2.80...2.73] [3.32...3.25] [6.88...6.84] [6.95...6.92] [6.97...6.95]	35.35 57.03 70.94 121.09 118.83 116.24	

(Continues)

TABLE 1 (Continued)

Metabolite (nanmoles)	Group	Structure	T ₁ (s)	T ₂ (s)	T ₁ /T ₂	Loss with J (Hz)	*δ ¹ H (ppm)	ppm range	*δ ¹³ C (ppm)
Ethanol (83.62 nmoles)	• ¹ CH ₃ • ² CH ₂	H ₃ C— ² OH	4.19 4.33	2.29 1.64	0.373 0.395	t (7.1Hz) q (7.1Hz)	1.19 3.66	[1.21...1.16] [3.69...3.62]	19.4 60.06
Ethanolamine (65.02 nmoles)	¹ CH ₂ • ² CH ₂	HO— ² — ¹ NH ₂	1.91 1.9	1.63 1.61	0.149 0.148	t (5.2Hz) t (5.2Hz)	3.14 3.82	[3.16...3.11] [3.85...3.79]	43.81 60.18
Formate (24.32 nmoles)	¹ CH		5.48	1.62	0.476	s	8.45	[8.46...8.44]	
Fumarate (63.96 nmoles)	• ¹ CH			7.05	6.70	0.540	s	6.52	[6.55...6.51]
GABA (gamma-aminobutyric acid) (61.23 nmoles)	¹ CH ₂ • ² CH ₂ ³ CH ₂			1.17 1.16 1.25	0.924 0.991 0.990	0.117 0.110 0.117	dd (7.7Hz; 7.4Hz) t (7.4Hz) t (7.7Hz)	1.90 2.30 3.00	[1.95...1.87] [2.33...2.27] [3.04...2.97]
Glutamate (49.4 nmoles)	¹ CH ₂ • ² CH ₂ ³ CH			0.681 0.749 1.72	0.582 0.651 1.26	0.150 0.139 0.142	m m dd (4.8Hz; 7.2Hz)	2.09 2.34 3.76	[2.17...2.02] [2.41...2.29] [3.79...3.74]
Glutamine (47.43 nmoles)	¹ CH ₂ • ² CH ₂ ³ CH			0.717 0.792 1.58	0.579 0.644 1.07	0.151 0.133 0.139	m m t (6Hz)	2.14 2.45 3.78	[2.17...2.11] [2.51...2.39] [3.81...3.76]
Glutathione (48.83 nmoles)	¹ CH ₂ ² CH ₂ ³ CH ₂ ⁴ CH ⁵ CH ₂ • ⁶ CH			0.474 0.517 0.348 0.446 0.291	0.339 0.242 0.236 0.275 0.159	m m m m m	2.17 2.56 2.95 3.79	[2.22...2.12] [2.63...2.49] [3.00...2.91] [3.82...3.75]	28.77 33.89 28.16 56.76
Glycerol (61.14 nmoles)	¹ CH ₂ • ² CH ₂ ³ CH			1.14 1.10 1.62	1.04 0.994 1.55	0.105 0.106 0.120	dd (5.5Hz; 6.6Hz) dd (6.5Hz; 11.8Hz) m	4.58 3.55 3.65 3.78	[4.61...5.56] [3.58...3.53] [3.68...3.62] [3.81...3.75]
Glycine (82.13 nmoles)	• ¹ CH ₂			2.05	1.85	0.159	s	3.56	[3.58...3.54]

(Continues)

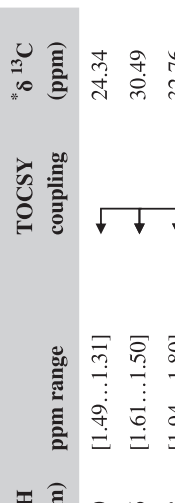
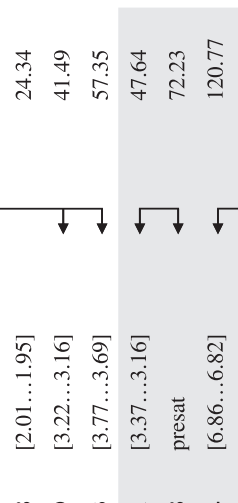
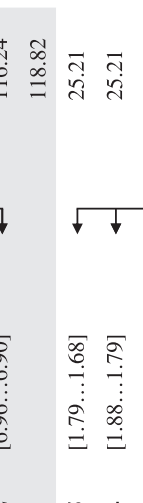
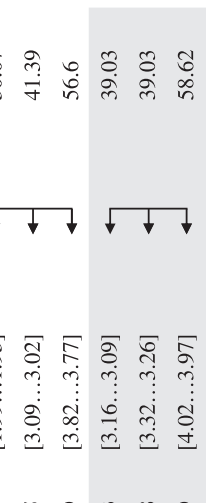
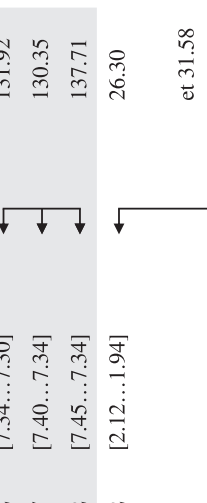
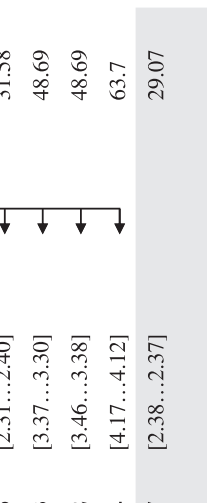
TABLE 1 (Continued)

TABLE 1 (Continued)

Metabolite (nmoles)	Group	Structure	T ₁ (s)	T ₂ (s)	T ₁ /T ₂	Loss with J (Hz)	*δ ¹ H (ppm)	*δ ¹³ C (ppm)	TOCSY coupling
Malate (50.47 nmoles)	• ¹ CH ₂		0.955	0.812	0.118	dd (15.4Hz; 10.4Hz)	2.37	[2.40...2.33]	↓
	¹ CH ₂		0.892	0.787	0.118	dd (15.4Hz; 2.9Hz)	2.67	[2.70...2.64]	↓
	³ CH		2.61	1.87	0.223	dd (10.4Hz; 2.9Hz)	4.31	[4.33...4.28]	↓
Mannitol (41.83 nmoles)	• ¹ CH ₂		0.851	0.479	0.182	dd (6.2Hz; 11.7Hz)	3.67	[3.71...3.63]	↓
	² CH		0.761	0.571	0.154	m	3.76	[3.78...3.72]	↓
	³ CH		0.843	0.680	0.133	d (8.9Hz)	3.79	[3.82...3.78]	↓
	⁴ CH ₂		0.77	0.434	0.196	dd (2.6Hz; 11.8Hz)	3.87	[3.91...3.85]	↓
Metformine (42 nmoles)	• ¹ CH ₃		1.52	1.08	0.133	s	3.05	[3.08...3.02]	39.87
Methionine (51.53 nmoles)	¹ CH ₂					m	2.13	[2.17...2.09]	↓
	• ² CH ₃					s			16.48
	¹ CH ₂					m	2.20	[2.27...2.17]	↓
	³ CH ₂					t (7.8Hz)	2.64	[2.67...2.61]	↓
	⁴ CH					dd (7.3Hz; 5Hz)	3.88	[3.90...3.86]	↓
Myo-inositol (53.38 nmoles)	¹ CH		1.24	0.936	0.121	t (9.5Hz)	3.27	[3.30...3.25]	↓
	² CH		1.14	0.873	0.12	dd (2.9Hz; 10Hz)	3.53	[3.56...3.50]	↓
	• ³ CH		1.41	1.04	0.126	dd (9.5Hz; 10Hz)	3.62	[3.65...3.59]	↓
	⁴ CH		1.19	0.924	0.118	t (2.9Hz)	4.05	[4.07...4.04]	↓
	⁵ CH								56.33
NAA (N-acetyl-L-aspartic acid) (39.91 nmoles)	• ¹ CH ₃		1.09	0.760	0.131	s	2.02	[2.05...1.99]	↓
	² CH ₂		0.559	0.457	0.186	dd (15.8Hz; 10.3Hz)	2.49	[2.54...2.46]	↓
	² CH ₂		0.546	0.463	0.183	dd (15.8Hz; 3.6Hz)	2.70	[2.74...2.67]	↓
	³ CH		1.91	1.27	0.162	dd (10.3Hz; 3.6Hz)	4.39	[4.42...4.37]	↓
NAG (N-acetyl-L-asparty-l-glutamic acid) (44.97 nmoles)	¹ CH ₂		0.431	0.222	0.344	m	1.90	[1.95...1.85]	↓
	¹ CH ₂					m	2.05	[2.12...2.00]	↓
	• ² CH ₃					s			30.99
	³ CH ₂					t (8.6Hz)	2.22	[2.26...2.18]	↓
	⁴ CH ₂					dd (9.9Hz; 16Hz)	2.53	[2.57...2.50]	↓
	⁴ CH ₂					dd (4.5Hz; 16Hz)	2.75	[2.79...2.72]	↓
⁵ CH						dd (4.6Hz; 8.6Hz)	4.13	[4.16...4.10]	58
	⁶ CH					dd (4.5Hz; 9.8Hz)	4.62	[4.65...4.59]	54.44

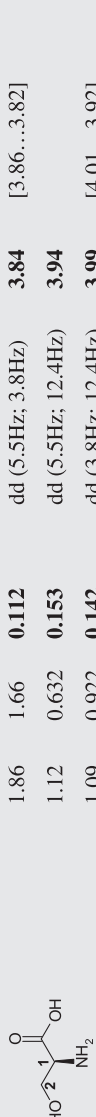
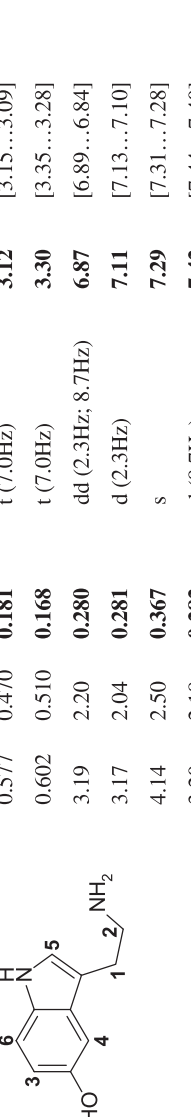
(Continues)

TABLE 1 (Continued)

Metabolite (nanmoles)	Group	Structure	T ₁ (s)	T ₂ (s)	T ₁ /T ₂	Loss with J (Hz)	*δ ¹ H (ppm)	ppm range	TOCSY coupling	*δ ¹³ C (ppm)
N-acetyl-L-lysine (35.57 nmoles)	¹ CH ₂		0.473	0.256	0.307	m	1.40	[1.49...1.31]	↔	24.34
	• ² CH ₂		0.468	0.289	0.277	m	1.56	[1.61...1.50]	↔	30.49
	³ CH ₂		0.491	0.325	0.251	m	1.88	[1.94...1.80]	↔	32.76
	⁴ CH ₃		1.20	0.759	0.138	s	1.98	[2.01...1.95]	↔	24.34
	⁵ CH ₂		0.500	0.283	0.282	t (6.7Hz)	3.19	[3.22...3.16]	↔	41.49
	⁶ CH		0.953	0.338	0.249	m	3.73	[3.77...3.69]	↔	57.35
Norepinephrine (48.8 nmoles)	¹ CH ₂		0.675	0.469	0.182	m	3.21	[3.37...3.16]	↔	47.64
	² CH		2.11	1.27	0.185	m	4.88	presat	↔	72.23
	³ CH					dd (2.3Hz; 8.2Hz)	6.84	[6.86...6.82]	↔	120.77
	• ⁴ CH					m	6.92	[6.96...6.90]	↔	116.24
	⁵ CH					m				118.82
Ornithine (40.00 nmoles)	¹ CH ₂		0.599	0.411	0.204	m	1.75	[1.79...1.68]	↔	25.21
	• ¹ CH ₂		0.598	0.422	0.200	m	1.84	[1.88...1.79]	↔	25.21
	² CH ₂		0.574	0.425	0.198	m	1.94	[1.99...1.93]	↔	30.07
	³ CH ₂		0.701	0.502	0.172	t (7.6Hz)	3.05	[3.09...3.02]	↔	41.39
	⁴ CH		1.31	0.785	0.143	t (6Hz)	3.79	[3.82...3.77]	↔	56.6
Phenylalanine (62.96 nmoles)	¹ CH ₂		0.492	0.426	0.198	dd (7.9Hz; 14.5Hz)	3.13	[3.16...3.09]	↔	39.03
	¹ CH ₂		0.512	0.413	0.203	dd (5.1Hz; 14.5Hz)	3.28	[3.32...3.26]	↔	39.03
	² CH		1.38	0.996	0.126	dd (5.1Hz; 7.9Hz)	3.99	[4.02...3.97]	↔	58.62
	³ CH		1.5	1.26	0.120	m	7.32	[7.34...7.30]	↔	131.92
	⁴ CH		1.59	1.24	0.130	m	7.37	[7.40...7.34]	↔	130.35
	⁵ CH		1.57	1.22	0.129	m	7.42	[7.45...7.34]	↔	137.71
Proline (47.99 nmoles)	¹ CH ₂					m	2.02	[2.12...1.94]	↔	26.30
	² CH ₂		1.71	1.53	0.130	m			et 31.58	
	² CH ₂		1.7	1.21	0.143	m	2.36	[2.31...2.40]	↔	31.58
	• ³ CH ₂		1.57	0.955	0.147	m	3.33	[3.37...3.30]	↔	48.69
	³ CH ₂		2.67	1.87	0.230	dd (6.2Hz; 8.5Hz)	3.42	[3.46...3.38]	↔	48.69
	⁴ CH						4.14	[4.17...4.12]	↔	63.7
Pyruvate (66.63 nmoles)	¹ CH ₃		4.7	4.65	0.402	s	2.37	[2.38...2.37]	↔	29.07

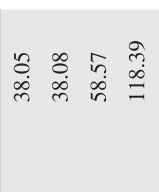
(Continues)

TABLE 1 (Continued)

Metabolite (nanmoles)	Group	Structure	T ₁ (s)	T ₂ (s)	T ₁ /T ₂	Loss with J (Hz)	[*] δ ¹ H (ppm)	ppm range	TOCSY coupling	* δ ¹³ C (ppm)
Scyllo-inositol (36.39 nmoles)	¹ CH		1.4	0.929	0.134	s	3.34	[3.36...3.32]		76.19
Serine (58.8 nmoles)	¹ CH			1.86	1.66	0.112	dd (5.5Hz; 3.8Hz)	3.84	[3.86...3.82]	58.96
	² CH ₂			1.12	0.632	0.153	dd (5.5Hz; 12.4Hz)	3.94		62.84
	• ² CH ₂			1.09	0.922	0.142	dd (3.8Hz; 12.4Hz)	3.99	[4.01...3.92]	
Serotonin (55.73 nmoles)	¹ CH ₂		0.577	0.470	0.181	t (7.0Hz)	3.12	[3.15...3.09]	↓	25.32
	² CH ₂			0.602	0.510	0.168	t (7.0Hz)	3.30	[3.35...3.28]	↓
	³ CH			3.19	2.20	0.280	dd (2.3Hz; 8.7Hz)	6.87	[6.89...6.84]	↓
	• ⁴ CH			3.17	2.04	0.281	d (2.3Hz)	7.11	[7.13...7.10]	↓
	⁵ CH			4.14	2.50	0.367	s	7.29	[7.31...7.28]	↓
	⁶ CH			3.20	2.18	0.282	d (8.7Hz)	7.42	[7.44...7.40]	↓
Succinate (49.83 nmoles)	• ¹ CH ₂		1.32	1.17	0.109	s	2.41	[2.44...2.37]		36.78
Taurine (41.44 nmoles)	¹ CH ₂		1.64	1.36	0.129	t (6.6Hz)	3.27	[3.29...3.24]	↓	50.15
	• ² CH ₂			1.64	1.34	0.130	t (6.6Hz)	3.42	[3.44...3.40]	↓
Threonine (48.85 nmoles)	• ¹ CH ₃		0.596	0.380	0.219	d (6.6Hz)	1.33	[1.36...1.30]	↓	22.12
	² CH			1.95	1.06	0.179	d (4.8Hz)	3.59	[3.60...3.57]	↓
	³ CH			1.64	0.464	0.238	dd (6.6Hz; 4.8Hz)	4.26	[4.29...4.23]	↓
Tryptophan (36.06 nmoles)	¹ CH ₂		0.483	0.350	0.235	dd (7.9Hz; 15.2Hz)	3.31	[3.35...3.28]	↓	28.71
	¹ CH ₂			0.482	0.314	0.258	dd (4.5Hz; 15.2Hz)	3.49	[3.53...3.46]	↓
	² CH			1.56	0.692	0.178	dd (4.5Hz; 7.9Hz)	4.06	[4.09...4.04]	↓
	³ CH			1.73	1.64	0.128	m	7.20	[7.22...7.17]	↓
	⁴ CH			1.95	1.51	0.149	m	7.28	[7.31...7.26]	↓
	⁵ CH			3.73	1.78	0.340	s	7.32	[7.33...7.26]	↓
	• ⁶ CH			2.35	1.13	0.219	m	7.54	[7.56...7.52]	↓
	⁷ CH			2.08	1.67	0.167	m	7.73	[7.76...7.72]	↓

(Continues)

TABLE 1 (Continued)

Metabolite (nanmoles)	Group	Structure	T ₁ (s)	T ₂ (s)	T ₁ /T ₂	Loss with J (Hz)	*δ ¹ H (ppm)	ppm range	TOCSY coupling	*δ ¹³ C (ppm)
Tyrosine (37.87 nmoles)	¹ CH ₂		0.442	0.378	0.220	dd (7.7Hz; 14.6Hz)	3.06	[3.10...3.02]	↓	38.05
	¹ CH ₂		0.422	0.373	0.222	dd (5.2Hz; 14.6Hz)	3.20	[3.23...3.17]	↓	38.08
	² CH		1.41	0.943	0.134	dd (5.2Hz; 7.8Hz)	3.94	[3.97...3.91]	↓	58.57
	³ CH		2.10	1.56	0.172	d (8.5Hz)	6.89	[6.92...6.87]	↓	118.39
	⁴ CH		1.45	1.19	0.119	d (8.5Hz)	7.18	[7.21...7.16]	↓	133.41
	[•] CH		4.44	3.64	0.384	d (7.7Hz)	5.80	[5.84...5.77]	↓	103.84
Uracil (64.11 nmoles)	¹ CH		4.32	3.87	0.374	d (7.7Hz)	7.54	[7.57...7.52]	↓	146.22
	² CH									
Valine (48.98 nmoles)	¹ CH ₃			0.718	0.656	0.135	d (7Hz)	0.99	[1.01...0.97]	↓
	[•] ² CH ₃			0.683	0.612	0.143	d (7Hz)	1.04	[1.07...1.03]	↓
	³ CH			1.22	1.01	0.113	m	2.28	[2.35...2.23]	↓
	⁴ CH			2.03	1.590	0.163	d (4.3Hz)	3.61	[3.63...3.60]	↓
β-Fructofuranose (87.14 nmoles)	¹ CH ₂						3.56	[3.62...3.52]	↓	65.20
	² CH ₂						3.80	[3.81...3.79]		72.46
	³ CH						3.79	[3.80...3.78]	↓	83.35
	¹ CH ₂						3.82	[3.82...3.78]	↓	65.20
	⁴ CH						3.83	[3.85...3.80]	↓	70.20
	⁵ CH			1.50	1.36	0.115	m	4.12	[4.13...4.11]	↓
α-Glucose (27.90 nmoles)	¹ CH						3.41	[3.44...3.37]	↓	72.1
	² CH			1.34	0.948	0.127	dd (9.8Hz; 3.8Hz)	3.53	[3.57...3.51]	↓
	³ CH						3.71	[3.74...3.68]	↓	73.89
	⁴ CH ₂						m	3.83	[3.84...3.81]	↓
	⁴ CH ₂						m	3.85	[3.87...3.84]	↓
	⁶ CH			1.68	1.34	0.134	d (3.7Hz)	5.24	[5.25...5.22]	↓
β-Fructopyranose (168 nmoles)	¹ CH ₂						3.56	[3.61...3.52]	↓	66.55
	⁵ CH ₂						3.69	[3.74...3.64]	↓	66.48
	² CH						3.79	[3.81...3.77]	↓	72.46
	[•] ³ CH									72.08
	⁴ CH						m	4.00	[4.01...3.93]	↓
	⁵ CH ₂						dd (1.2Hz; 12.7Hz)	4.03	[4.05...4.01]	↓

(Continues)

TABLE 1 (Continued)

Metabolite (nanmoles)	Group	Structure	T ₁ (s)	T ₂ (s)	Loss with T ₁ /T ₂	*δ ¹ H (ppm)	ppm range	TOCSY coupling	*δ ¹³ C (ppm)
β-Glucose (34.16 nmoles)	¹ CH		1.50	1.11	0.129	dd (9Hz; 7.7Hz)	3.24	[3.28...3.21]	76.74
	² CH				m	3.41	[3.44...3.37]	72.1	
	³ CH				m	3.47	[3.48...3.45]	78.43	
	⁴ CH				dd (12.3Hz; 5.6Hz)	3.49	[3.51...3.48]	78.42	
	⁵ CH ₂				dd (12.2Hz; 2Hz)	3.76	[3.80...3.74]	63.2	
	⁵ CH ₂				dd (12.2Hz; 2Hz)	3.89	[3.92...3.89]	63.2	
	• ⁶ CH		1.12	0.907	0.115	d (7.9Hz)	4.65	[4.67...4.64]	98.56
(b) Compounds with ³¹P									
Metabolite (nanmoles)	Group	Structure	T ₁ (s)	T ₂ (s)	Loss with T ₁ /T ₂	*δ ¹ H *δs ³¹ P (ppm)	ppm range	TOCSY coupling	*δ ¹³ C (ppm)
ATP (adenosine triphosphate) (50.68 nmoles)	¹ CH ₂		0.526	0.197	0.379	m	4.21	[4.24...4.18]	64.76
	¹ CH ₂				0.394	m	4.30	[4.34...4.23]	64.76
	² CH				0.244	m	4.41	[4.44...4.39]	83.64
	³ CH				0.256	dd (3.6Hz; 5Hz)	4.63	[4.67...4.61]	70.05
	⁴ CH				0.210	dd (4.6Hz; 6.1Hz)	4.82	[4.86...4.80]	73.93
	• ⁵ CH				0.208	d (6Hz)	6.15	[6.17...6.13]	86.23
	⁶ CH				0.352	s	8.25	[8.27...8.29]	
	⁷ CH				0.153	s	8.55	[8.58...8.54]	139.6
	¹ P				d (19.1Hz)	-2.63	[−2.5...−2.72]		
	² P				d (19.1Hz)	-7.49	[−7.41...−7.6]		
	³ P				t (19.1Hz)	-17.95	[−17.8...−18.1]		
Glycerophosphocholine (52.68 nmoles)	¹ CH ₃		0.59	0.455	0.187	s	3.24	[3.26...3.22]	56.56
	² CH ₂				0.178	dd (6Hz; 12Hz)	3.65	[3.65...3.58]	64.42
	² CH ₂				m	3.70	[3.73...3.65]	64.42	
	³ CH ₂				m	3.92	[3.99...3.84]	68.54	
	⁴ CH ₂				0.156	m	4.33	[4.37...4.30]	69.16
	⁵ CH				s	3.33	[−3.36...−3.29]	73.29	
	• ⁶ CH ₂								62.09
	¹ P								

(Continues)

TABLE 1 (Continued)

Metabolite (nanomoles)	Group	Structure	T ₁ (s)	T ₂ (s)	J (Hz)	Loss with T ₁ /T ₂	*δ ¹ H*δs ³¹ P (ppm)	ppm range	TOCSY coupling	HMBC coupling	*δ ¹³ C (ppm)
NAD (nicotina- mide)	¹ CH ₂					m	4.25	[4.31...4.19] [4.40...4.36]	↓	68.00 67.36	
adenine	² CH					m	4.38	[4.44...4.40]	↓	72.86	
dinucleo- tide) (64.8 nmoles)	³ CH					dd (3Hz; 5Hz)	4.42	[4.49...4.45]	↓	79.98	
	⁴ CH					t (5Hz)	4.47	[4.54...4.48]	↓	72.86	
	⁵ CH					dd (3Hz; 5Hz)	4.52	[4.56...4.52]	↓	89.36	
	⁶ CH					m	4.53	[4.82...4.76]	↓	76.42	
	⁷ CH					t (5.8Hz)	4.78	[6.04...6.05]	↓	89.04	
	⁸ CH					1.66	0.805	0.171	d (6.2Hz)	6.02	
	⁹ CH					1.11	0.586	0.163	d (5.2Hz)	6.07	
	¹⁰ CH					2.33	0.918	0.232	s	8.14	
	¹¹ CH					1.92	0.706	0.211	dd (6.4Hz; 8Hz)	8.20	
	¹² CH					1.49	0.770	0.160	s	8.40	
	¹³ CH					1.9	0.924	0.184	d (8.3Hz)	8.83	
	¹⁴ CH					1.31	0.625	0.168	d (6.1Hz)	9.15	
	• ¹⁵ CH					1.51	0.879	0.149	s	9.33	
	¹ P								d (20Hz)	-7.87	
	² P								d (20Hz)	-8.22	
										[−8.13...−8.01]	
										[−8.13...−8.31]	
NADH (reduced nicotina- mide)	¹ CH ₂					0.157	0.450	dd (3.6Hz; 18Hz)	2.56	[2.61...2.52]	
adenine	² CH ₂					0.529	0.178	0.409	m	2.72	[2.76...2.68]
dinucleo- tide) (65.21 nmoles)	³ CH								m	4.10	[4.14...4.03]
	⁴ CH								dd (5.5; 7.3Hz)	4.17	[4.20...4.15]
	⁵ CH ₂								dd (1.6; 5.4Hz)	4.23	[4.26...4.20]
	⁶ CH ₂								m	4.28	[4.31...4.26]
	⁷ CH								m	4.39	[4.41...4.36]
	⁸ CH								t (4.1Hz)	4.51	[4.55...4.48]
	⁹ CH								t (5.15Hz)	4.70	[4.72...4.68]
	¹⁰ CH								m	4.73	[4.75...4.71]
	¹¹ CH								d (7.4Hz)	4.77	[4.78...4.76]
	¹² CH									5.94	[5.98...5.91]
	• ¹³ CH									6.13	[6.17...6.10]
	¹⁴ CH									6.90	[6.93...6.88]
	¹⁵ CH									8.22	[8.23...8.20]
	¹⁶ CH									8.48	[8.51...8.46]
	¹ P									-8.01	[−7.95...−8.07]

(Continues)

TABLE 1 (Continued)

Metabolite (nanomoles)	Group	Structure	T ₁ (s)	T ₂ (s)	Loss with T ₁ /T ₂	J (Hz)	*δ ¹ H*δs ³¹ P (ppm)	ppm range	TOCSY coupling	HMBC coupling	*δ ¹³ C (ppm)
NADP (nicotina- mide adenine dinucleotide phosphate) (36.43 nmoles)	¹ CH ₂ ² CH ³ CH ⁴ CH ⁵ CH ⁶ CH ⁷ CH ⁸ CH ⁹ CH ¹⁰ CH ¹¹ CH ¹² CH ¹³ CH ¹⁴ CH ¹⁵ CH ¹ P ² P ³ P				m		4.21 [4.26...4.18] 4.32 [4.35...4.28]			67.7 67.67	
					m	dd (2.7Hz; 5Hz)	4.40 [4.42...4.36]			73.20	
					t (5.2Hz)		4.44 [4.49...4.42]			85.50	
					m		4.49 [4.51...4.46]			80.32	
					t (4.6Hz)		4.63 [4.66...4.62]			89.37	
					m		4.97 presat			72.55	
										78.7	
										102.7	
										88.73	
NADPH (reduced nicotina- mide adenine dinucleotide phosphate) (65.99 nmoles)	¹ CH ₂ ² CH ³ CH ⁴ CH ⁵ CH ⁶ CH ₂ ⁷ CH ₂ ⁸ CH ⁹ CH ¹⁰ CH ¹¹ CH ¹² CH ¹³ CH ¹⁴ CH ¹⁵ CH ¹⁷ CH ¹ P ² P				m		0.430 dd (3.6Hz; 18Hz)	2.63 [2.69...2.59]		21.52	
					m		0.428 m	2.78 [2.83...2.74]		65.52	
					m			4.07 [4.12...4.00]		82.02	
					m	dd (5.4Hz; 7.5Hz)	4.16 [4.19...4.14]			70.37	
					m		4.22 [4.25...4.19]			70.37	
					m		4.31 [4.35...4.28]			64.87	
					m		4.40 [4.43...4.37]			64.87	
					t (4.3Hz)		4.60 [4.63...4.57]			82.67	
					m		4.75 [4.78...4.72]			69.73	
					d (7.5Hz)		4.94 [4.96...4.91]			94.64	
					d (1.6; 8.4Hz)		5.92 [5.95...5.88]			122.8	
					d (4.7Hz)		6.21 [6.24...6.18]			86.23	
										138.3	
										139.3	

(Continues)

TABLE 1 (Continued)

Metabolite (nanmoles)	Group	Structure	Loss			* $\delta^1\text{H}$ * $\delta^3\text{P}$ (ppm)	TOCSY coupling	HMBC coupling	${}^3\delta^{13}\text{C}$ (ppm)
			T ₁ (s)	T ₂ (s)	T ₁ /T ₂				
PEP (phospho- enolpyruvic acid) (40.43 nmoles)	¹ CH ₂ [•] CH ₂ ¹ P		0.486 0.645	0.193 0.313	0.204 0.385	m m	5.19 5.38	[5.21...5.18] [5.40...5.37]	102.9 102.9
Phospho-cho- line (42.95 nmoles)	¹ CH ₃ ² CH ₂ [•] CH ₂ ¹ P		0.647	0.526	0.164	s	3.23	[3.25...3.21]	56.54
Phospho-cré- atine (26.08 nmoles)	¹ CH ₃ ² CH ₂ ¹ P		0.721 0.823	0.635 0.707	0.139 0.128	m m	3.61 4.16	[3.63...3.59] [4.20...4.13]	69.00 60.57
						s	6.65	[6.68...6.62]	

All metabolite solutions were prepared in D₂O containing 9.4 mM of PBS (pH 7.4) and 0.125 w/v% TSP.

Presaturation: the water signal presaturation scheme used in the experiment made it not possible to determine the ppm range of this multiplet.

♦Referenced to PBS (H₂PO₄⁻/HPO₄²⁻) (buffer) at 5.36 ppm.

Abbreviations: s = singlet; d = doublet; t = triplet; m = multiplet; dd = doublet of doublet; q = quadruplet.

*Referenced to TSP (3-(trimethylsilyl) propionic-2,2,3,3-d4 acid, sodium salt) at 0.00 ppm in ¹H and -0.25 ppm in ¹³C.

•Group has been defined as cluster 0 in Chenomex.

and ^1H - ^{13}C HSQC.¹⁶ For metabolites containing phosphorus, additional experiments were also recorded: 1D ^{31}P with ^1H decoupling and 2D ^1H - ^{31}P HMBC experiment (see Supporting Information).

2.2.1 | Relaxation times measurements were performed after the two 1D sequences

Transverse relaxation times were measured using a pseudo 2D ^1H Carr-Purcell-Meiboom-Gill (CPMG) pulse sequence with presaturation. This experiment consists in the acquisition of several 1D spectra with an increasing length of CPMG times. The experiment was performed with the following parameters: spectral width 14.0 ppm, number of points 32 k, relaxation delay 2 seconds, acquisition time 2.33 seconds, and 64 scans. Total acquisition time was of 1 hour 26 minutes.

Longitudinal relaxation times were measured using a pseudo 2D ^1H inversion recovery pulse sequence with water suppression, which consists in the acquisition of several 1D spectra with an increasing relaxation delay after the 180° pulse was used. A CPMG module of 93 ms was added just before the acquisition time in order to reduce broad spectral features, which arise from lipids and macromolecules. The experiment was performed with the following parameters: spectral width 14.0 ppm, number of points 32 k, relaxation delay 8 seconds, acquisition time 2.33 seconds, and 64 scans. Total acquisition time was 2 hours and 6 minutes.

2.3 | HRMAS NMR data processing

All spectra of the metabolic database were processed using Topspin 3.5 (Bruker BioSpin) and calibrated with respect to the TSP signal at 0.00 ppm in ^1H and at -0.25 ppm in ^{13}C . Phosphorus spectra were referenced to the ^{31}P signal of the PBS ($\text{H}_2\text{PO}_4^-/\text{HPO}_4^{2-}$) buffer at 5.36 ppm.

2.3.1 | Processing and analysis of 2D relaxation data

For both T_1 and T_2 analysis, the free induction decays were first multiplied with a cosine squared weighting function before Fourier transformation. Data were then carefully phased and baseline corrected. The resulting data were analyzed using the Dynamics Center 2.2.4 package, which is a module of Topspin 3.5 and which is able to perform advanced mono- and biexponential curve fitting. This software fits relaxation data using a combination of *Simplex* and *Levenberg-Marquardt* algorithms.

2.4 | Quantitative aspects

2.4.1 | Correction factors to take into account T_1 and T_2 effects for a more accurate quantification in CPMG experiments

The signal measured after a CPMG sequence when taking into account T_1 and T_2 relaxation is given by (Equation 1):

$$S_{Measured} = S_o \left(1 - \exp \left(-\frac{t_a}{T_1} \right) \right) \times \exp \left(-\frac{t_b}{T_2} \right) \quad (1)$$

where S_o is the true intensity of the signal.

The signal loss is therefore given by (Equation 2):

$$S_{Loss} = S_o \left(1 - \left(1 - \exp \left(-\frac{t_a}{T_1} \right) \right) \exp \left(-\frac{t_b}{T_2} \right) \right) \quad (2)$$

where t_a is the acquisition time plus the recycle time and t_b is the length of the CPMG element. Under our experimental conditions: $t_a = 4.33$ seconds and $t_b = 93.71$ ms.

The correction factor that should be used to correct for the relaxation effects is therefore (Equation 3):

$$C_{Factor} = 1 / \left[\left(1 - \exp \left(-\frac{t_a}{T_1} \right) \right) \times \exp \left(-\frac{t_b}{T_2} \right) \right] \quad (3)$$

2.5 | Human brain tumor specimens

Six human brain specimens (normal cerebral cortex [$n = 2$], oligodendrogloma [$n = 2$], and glioblastoma [$n = 2$]) were prepared following our standard protocol in order to evaluate the performances of our database for metabolite assignment. Additionally, the T_1 and T_2 relaxation times of 17 brain metabolites (20 chemical groups) were determined in these samples. These relaxation times were measured to confirm the applicability of our database to biological samples.

3 | RESULTS

For each of the 76 metabolites contained in the database, the full set of experiments described in Methods was acquired. The 1D and 2D spectra were manually assigned using the information contained in the different spectra as well as the Human Metabolome Database⁹ and simulated NMR spectra.¹⁷ The complete list of ^1H / ^{13}C chemical shifts and ^1H - ^1H J-couplings for the 76 metabolites is presented in Table 1. It also lists the T_1 and T_2 values of the different protons of

the molecules in the metabolic database. An example of the T_1/T_2 measurement for the different signals of ascorbate is shown in Figure 1. As expected for small molecules in solution, the values of the T_1 and T_2 are very similar. However, some protons like the Lactate_CH exhibit a distinct behavior, with T_2 being much shorter than T_1 . These relaxation parameters are particularly important because they allow to estimate the amount of magnetization lost because of relaxation and to compute a correction factor. The comparison of the T_1/T_2 values obtained for the metabolites in solution and in biopsy samples is presented in Table 2. For all metabolites, both T_1 and T_2 values in biopsy specimens are slightly shorter than in solution. On average, the T_1 values obtained in biopsy samples are 17.3% shorter whereas the T_2 values are 27.2% shorter. The average loss of magnetization attributed to T_1/T_2 relaxation effects during a CPMG experiment

is computed to be 16% in solution and 17% in biopsy specimens. This result is quite remarkable and provides, for the first time, an estimate of the correction factor that should be used to obtain a more accurate quantification. The fact that the correction factors are so similar, despite slight variations in T_1 and T_2 , can be explained using Equation . A shorter T_1 will decrease signal loss, whereas a shorter T_2 will increase it. The simultaneous decrease of T_1 and T_2 in biopsy specimens explains that similar signal losses are observed. These values are applicable, provided our own experimental conditions are followed (i.e., CPMG block of 93 ms and recovery delay of 4.33 seconds). However, the T_1 and T_2 values presented in Table 1 allow to estimate the loss in signal for any of these 2 experimental parameters. As a validation sample, we have used 4 mixtures at different concentrations of 4 metabolites. The results presented in Figure 2 show that a high precision

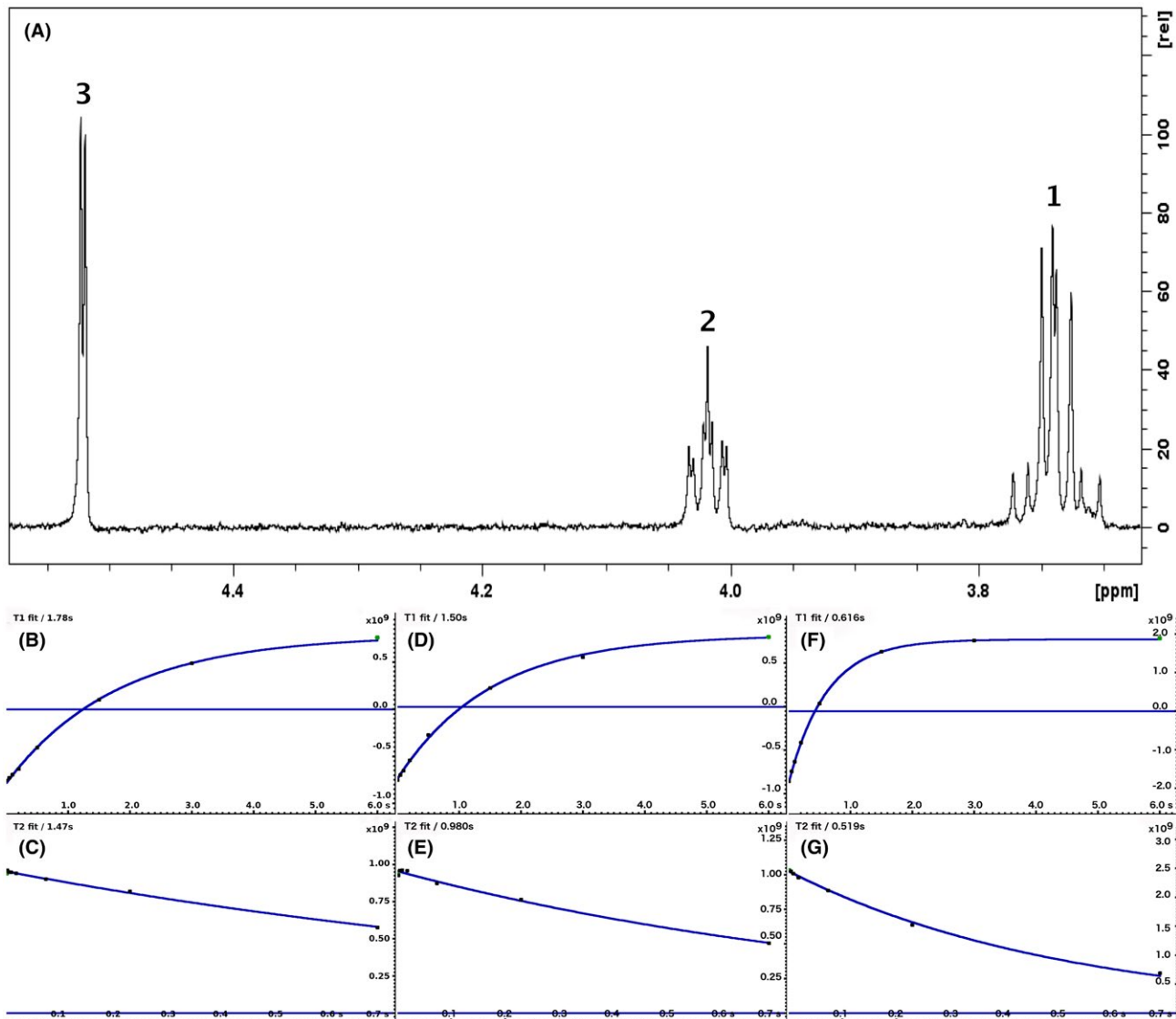


FIGURE 1 A 500-MHz 1D ^1H CPMG HRMAS spectrum of ascorbate along with graphs showing the measurement of T_1 and T_2 for the 3 different chemical groups (peak 3 at 4.52 ppm: b and c; peak 2 at 4.02 ppm: d and e; peak 1 at 3.74 ppm: f and g)

TABLE 2 T_1 and T_2 relaxation times measured for 17 metabolites and 20 chemical groups on 6 different biopsies: normal cerebral cortex ($n = 2$), oligodendrogloma ($n = 2$), glioblastoma ($n = 2$)

	Biopsy T_1 (s)	Solution T_1 (s)	Biopsy T_2 (s)	Solution T_2 (s)	Biopsy CPMG signal loss	Solution CPMG signal loss
Acetate_1.92ppm	2.49 ± 0.15	3.20	1.42 ± 0.05	2.61	0.23 ± 0.02	0.28
Alanine_1.48ppm	0.92 ± 0.02	1.05	0.70 ± 0.04	0.83	0.13 ± 0.01	0.12
Ascorbate_4.52ppm	1.17 ± 0.03	1.78	0.63 ± 0.07	1.47	0.16 ± 0.01	0.14
Choline_3.22ppm	1.27 ± 0.08	1.45	1.09 ± 0.06	1.15	0.11 ± 0.01	0.11
Creatine_3.94ppm	0.71 ± 0.03	0.80	0.57 ± 0.06	0.69	0.15 ± 0.01	0.13
Creatine_3.03ppm	1.34 ± 0.05	1.49	0.89 ± 0.06	1.22	0.14 ± 0.01	0.12
GABA_1.90ppm	0.83 ± 0.06	1.17	0.40 ± 0.06	0.92	0.21 ± 0.02	0.12
Glutamate_2.09ppm	0.68 ± 0.02	0.68	0.39 ± 0.02	0.58	0.21 ± 0.01	0.15
Glutamine_2.14ppm	0.62 ± 0.01	0.72	0.45 ± 0.02	0.58	0.19 ± 0.01	0.15
Glutamine_2.45ppm	0.72 ± 0.02	0.79	0.55 ± 0.03	0.64	0.16 ± 0.01	0.14
Glycerophosphocholine_3.24ppm	0.57 ± 0.03	0.59	0.50 ± 0.02	0.46	0.18 ± 0.01	0.19
Glycine_3.56ppm	1.49 ± 0.05	2.05	0.89 ± 0.12	1.85	0.15 ± 0.01	0.16
Lactate_1.33ppm	0.99 ± 0.05	1.15	0.65 ± 0.06	0.77	0.15 ± 0.01	0.13
Lactate_4.12ppm	1.68 ± 0.14	3.43	0.53 ± 0.05	0.57	0.23 ± 0.01	0.39
Myo-Inositol_4.05ppm	0.83 ± 0.02	1.19	0.45 ± 0.02	0.92	0.19 ± 0.01	0.12
NAA_2.02ppm	1.02 ± 0.06	1.09	0.60 ± 0.05	0.76	0.16 ± 0.01	0.13
Phosphocholine_3.23ppm	0.62 ± 0.02	0.65	0.50 ± 0.02	0.53	0.17 ± 0.01	0.16
Taurine_3.42ppm	1.33 ± 0.09	1.64	0.81 ± 0.07	1.34	0.14 ± 0.01	0.13
Valine_1.04ppm	0.67 ± 0.06	0.68	0.52 ± 0.01	0.61	0.17 ± 0.00	0.14
Scyllo-Inositol_3.34ppm	0.87 ± 0.02	1.40	0.53 ± 0.03	0.93	0.17 ± 0.01	0.14

The value of T_1 and T_2 for the pure metabolite is also reported. The last 2 columns show the signal loss expected during a CPMG experiment for the 17 metabolites in a biopsy and in a pure solution, taking into account both T_1 and T_2 effects.

in the concentrations can be obtained, provided the corrections attributed to relaxation effects are taken into account.

4 | DISCUSSION

HRMAS NMR metabolomics is a promising technique to evaluate the metabolic status of the tissue of a patient. Depending on the tissue and the disease studied, different metabolic pathways and different metabolites may be affected.⁶⁻⁸ For instance, alterations in the following pathways have been studied by HRMAS: glycolysis, tricarboxylic acid cycle, glutamate/glutamine cycle, 1-carbon metabolism, membrane metabolism, and amino acid synthesis.

HRMAS NMR metabolomics has been shown to be potentially beneficial in personalized treatment in the following fields of medicine¹⁸⁻²⁰:

- (a) Evaluation of the quality of grafts in liver or lung transplants.^{5,21,22}
- (b) Detection of oncometabolites for identification of DNA mutations: 2-hydroxyglutarate in glioma for isocitrate

dehydrogenase mutation,²³ succinate in pheochromocytomas to distinguish succinate dehydrogenase (SDHx)- and non-SDHx-related tumors.²⁴

- (c) Detection of biomarkers to evaluate tumor aggressiveness. Past studies have shown which metabolic pathways are involved in tumor growth.^{3,25} In oligodendroglomas, the degree of tumor hypoxia obtained at an early state of disease was better correlated with the patient prognosis than the morphological criteria.⁴ Distinct metabolic signatures were found for lung adenocarcinoma (related to phospholipid metabolism and protein catabolism) and squamous-cell carcinoma (glycolytic and glutaminolytic profiles).²⁶ In pancreatic adenocarcinoma, the assessment of ethanolamine concentration can be clinically relevant as a single metabolic biomarker to predict long-term survival.⁶
- (d) Evaluation of tumor exeresis during surgery: The intraoperative metabolic analysis of biopsy specimens can help better characterize tumor margins. This novel application has been presented as a proof of concept in colon cancer.²⁷

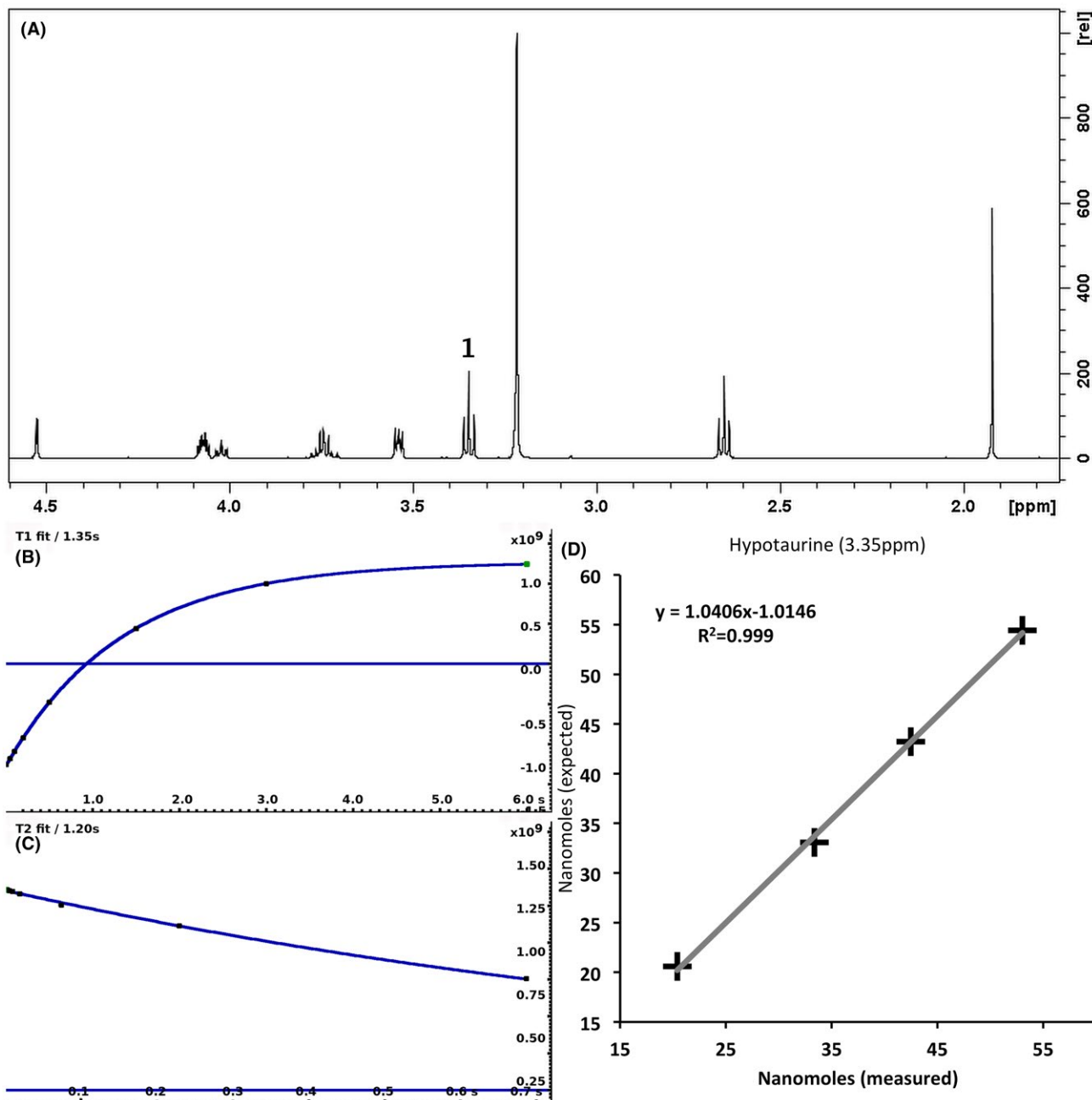


FIGURE 2 A 500-MHz 1D ¹H CPMG HRMAS spectrum of a mixture containing 4 metabolites (acetate, ascorbate, choline, and hypotaurine) (A) described in Methods. The measurement of T₁ (B) and T₂ (C) of hypotaurine at 3.35 ppm is shown. The graph (D) shows the correlation between the number of nanomoles measured and expected in the 4 different solutions for hypotaurine. The nanomoles measured values have been corrected for T₁ and T₂ effects

The simplified metabolite pathways used in our laboratory is presented in Supporting Information Figure S1. The analysis of the variations in concentration of the different metabolites is usually performed by multivariate or network analysis.²⁸ This approach allows to study the up- and downregulation of different pathways in order to find potential biomarkers. In this context, rapid and robust identification as well as reliable quantification are critical.

When performing a study by HRMAS NMR on a large cohort of samples, the detailed metabolite assignment is usually performed only on a few samples. For these samples, the combination of 1D and 2D NMR spectra is particularly powerful, and the database presented in this article makes this assignment relatively straightforward. A unique feature of our metabolic database is that it contains all the spectra used classically to study biopsy specimens: ¹H 1D,

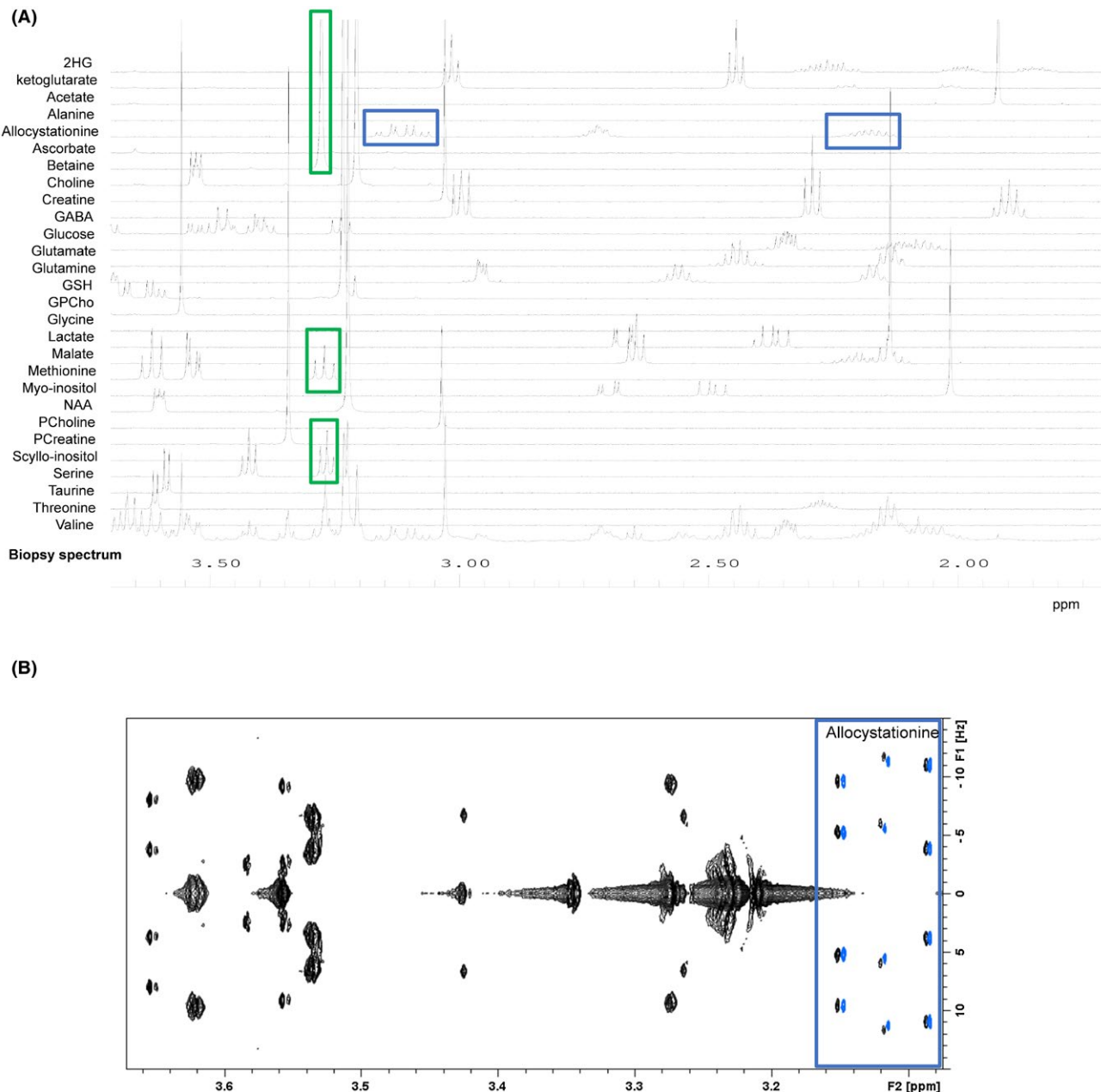


FIGURE 3 (A) A 500-MHz 1D ^1H CPMG HRMAS spectrum of a human brain tumor sample (right temporal glioblastoma) and several spectra of the database superimposed on top. The resonances of allocystathione are highlighted with blue squares. The green squares show the spectral region at 3.3 ppm, where there is a strong signal overlap that will require additional 2D experiments. (B) A 500-MHz 2D J-resolved HRMAS spectrum of a human brain tumor sample (right temporal glioblastoma) superimposed with the allocystathione spectrum (the spectrum has been slightly shifted to the right in order to visualize the good agreement between the peaks)

^1H 1D CPMG, 2D J-Resolved, 2D TOCSY, and 2D HSQC. Several softwares, like Metabominer²⁹ and AssureNMR (Bruker BioSpin) can provide a semiautomated identification using J-Resolved, TOCSY, and ^1H - ^{13}C HSQC spectra.²⁹ Once the different peaks have been assigned in these samples, the assignment can simply be reported in the 1D spectrum of the remaining samples. Because the conditions for sample preparation and data acquisition follow a strict protocol, there is little variation in peaks position attributed to pH or temperature. Our database was applied to analyze

multiple biopsy specimens obtained from tissue banks or from routine surgery. It is clearly a powerful tool that helps provide an accurate and fast metabolic profile. To illustrate this point, Figure 3A shows a typical example of the use of the database when assigning the 1D ^1H CPMG spectrum of a biopsy sample. The CPMG is the experiment that is used systematically to characterize biopsy specimens. In this example, the assignment of Allocystathione is highlighted. In case of severe overlap, the assignment can also be confirmed by superimposing the different 2D spectra

of the biopsy sample with the corresponding spectra of the database. Figure 3B illustrates this approach by showing the assignment of Allocystationine in the de 2D J-Resolved spectrum of a human biopsy. This approach allows to assign the different signals contained in a biopsy sample with a very high degree of confidence.

For biomedical applications, it is essential to obtain quantitative information on metabolites present in tissues, that is, in the cells, extracellular space, and microenvironment. This information is usually presented as the number of nmoles of metabolites per mg of biopsy material. The reliability of the analysis will depend on the quality of the tissue sample controlled in histopathology (with a preference for the HRMAS sample itself or the mirror sample). The T_1 and T_2 data presented in this article allow to improve the quantification of metabolites in biopsies by computing, for each chemical group of a given metabolite, a correction factor that takes into account relaxation losses during the CPMG experiment. Under our experimental CPMG conditions, this loss of signal ranges from 11% to 23%. Similar relaxation times measurements have been performed *in vivo* at 17.2T in the rat brain to improve quantification of metabolites.³⁰ A very important feature of our HRMAS database is that it contains spectra recorded on a known quantity of metabolites. This implies that the CPMG spectrum of the database can be used to directly estimate the amounts of metabolites contained in the CPMG spectrum of a biopsy sample. The scaling factor used to match the peaks in the biopsy spectrum can be used to calculate the concentration of that specific metabolite. Techniques of quantification of metabolites in biopsy specimens are becoming very performant; however, they still need to be improved, notably in terms of speed and automation. In our laboratory, these quantification routines are currently being implemented in the Chenomx and AssureNMR software. This database has the potential to become a reference to identify metabolite peaks in tissues outside our laboratory, provided data are collected under the exact experimental conditions. It should be useful at both 500 and 600 MHz, which are the 2 magnetic fields most commonly used in this type of study.

5 | CONCLUSION

HRMAS NMR metabolomics is becoming an important technique in clinical research and could potentially improve personalized medicine. The database presented in this study considerably simplifies the assignment of signals in the spectra of biopsy specimens. The spectra of the database are all provided along with the number of nmoles used for the standard sample, which makes them useful for quantification applications. Additionally, the loss of magnetization attributed to T_1 and T_2 effects observed during CPMG experiments

run under our experimental conditions is reported for metabolites in solution (average loss 16%) and in biopsy specimens (average loss 17%).

ACKNOWLEDGMENT

We thank Dr Clément Heude for his help in analyzing the T_1 and T_2 data of biopsy specimens.

REFERENCES

1. Griffin JL, Shockcor JP. Metabolic profiles of cancer cells. *Nat Rev Cancer*. 2004;4:551–561.
2. Claudino WM, Quattrone A, Biganzoli L, Pestrin M, Bertini I, Di Leo A. Metabolomics: available results, current research projects in breast cancer, and future applications. *J Clin Oncol*. 2007;25:2840–2846.
3. Bathan TF, Sitter B, Sjøbakk TE, Tessem MB, Gribbestad IS. Magnetic resonance metabolomics of intact tissue: a biotechnological tool in cancer diagnostics and treatment evaluation. *Cancer Res*. 2010;70:6692–6696.
4. Erb G, Elbayed K, Piotto M, et al. Toward improved grading of malignancy in oligodendrogiomas using metabolomics. *Magn Reson Med*. 2008;59:959–965.
5. Faitot F, Besch C, Battini S, et al. Impact of real-time metabolomics in liver transplantation: graft evaluation and donor-recipient matching. *J Hepatol*. 2018;68:699–706.
6. Battini S, Faitot F, Imperiale A, et al. Metabolomics approaches in pancreatic adenocarcinoma: tumor metabolism profiling predicts clinical outcome of patients. *BMC Med*. 2017;15:56.
7. Battini S, Imperiale A, Taïeb D, et al. High-resolution magic angle spinning (^1H) nuclear magnetic resonance spectroscopy metabolomics of hyperfunctioning parathyroid glands. *Surgery*. 2016;160:384–394.
8. Imperiale A, Battini S, Averous G, et al. In vivo detection of catecholamines by magnetic resonance spectroscopy: a potential specific biomarker for the diagnosis of pheochromocytoma. *Surgery*. 2016;159:1231–1233.
9. Wishart DS, Jewison T, Guo AC, et al. HMDB 3.0—The Human Metabolome Database in 2013. *Nucleic Acids Res*. 2013;41:D801–D807.
10. Julià-Sapé M, Acosta D, Mier M, Arús C, Watson D; INTERPRET consortium. A multi-centre, web-accessible and quality control-checked database of *in vivo* MR spectra of brain tumour patients. *MAGMA*. 2006;19:22–33.
11. Julià-Sapé M, Lurgi M, Mier M, et al. Strategies for annotation and curation of translational databases: the eTUMOUR project. *Database (Oxford)*. 2012;2012:bas035.
12. Wider G, Dreier L. Measuring protein concentrations by NMR spectroscopy. *J Am Chem Soc*. 2006;128:2571–2576.
13. Aue WP, Karhan J, Ernst RR. Homonuclear broad-band decoupling and 2-dimensional J-resolved NMR spectroscopy. *J Chem Phys*. 1976;64:4226–4227.
14. Braunschweiler L, Ernst R. Coherence transfer by isotropic mixing: application to proton correlation spectroscopy. *J Magn Reson*. 1983;53:521–528.
15. Kupce E, Keifer PA, Delepiere M. Adiabatic TOCSY MAS in liquids. *J Magn Reson*. 2001;148:115–120.

16. Davis AL, Laue ED, Keeler J, Moskau D, Lohman J. Experiments for recording pure-absorption heteronuclear correlation spectra using pulsed field gradients. *J Magn Reson.* 1991;94:637–644.
17. Binev Y, Marques MM, Aires-de-Sousa J. Prediction of 1H NMR coupling constants with associative neural networks trained for chemical shifts. *J Chem Inf Model.* 2007;47:2089–2097.
18. Armitage EG, Southam AD. Monitoring cancer prognosis, diagnosis and treatment efficacy using metabolomics and lipidomics. *Metabolomics.* 2016;12:146.
19. Vander Heiden MG. Targeting cancer metabolism: a therapeutic window opens. *Nat Rev Drug Discov.* 2011;10:671–684.
20. Everett JR. NMR-based pharmacometabonomics: a new paradigm for personalised or precision medicine. *Prog Nucl Magn Reson Spectrosc.* 2017;102–103:1–14.
21. Duarte IF, Stanley EG, Holmes E, et al. Metabolic assessment of human liver transplants from biopsy samples at the donor and recipient stages using high-resolution magic angle spinning 1H NMR spectroscopy. *Anal Chem.* 2005;77:5570–5578.
22. Benahmed MA, Santelmo N, Elbayed K, et al. The assessment of the quality of the graft in an animal model for lung transplantation using the metabolomics 1H high-resolution magic angle spinning NMR spectroscopy. *Magn Reson Med.* 2012;68:1026–1038.
23. Choi C, Ganji SK, DeBerardinis RJ, et al. 2-hydroxyglutarate detection by magnetic resonance spectroscopy in IDH-mutated patients with gliomas. *Nat Med.* 2012;18:624–629.
24. Imperiale A, Moussallieh F-M, Roche P, et al. Metabolome profiling by HRMAS NMR spectroscopy of pheochromocytomas and paragangliomas detects SDH deficiency: clinical and pathophysiological implications. *Neoplasia.* 2015;17:55–65.
25. Loening NM, Chamberlin AM, Zepeda AG, Gonzalez RG, Cheng LL. Quantification of phosphocholine and glycerophosphocholine with 31P edited 1H NMR spectroscopy. *NMR Biomed.* 2005;18:413–420.
26. Rocha CM, Barros AS, Goodfellow BJ, et al. NMR metabolomics of human lung tumours reveals distinct metabolic signatures for adenocarcinoma and squamous cell carcinoma. *Carcinogenesis.* 2015;36:68–75.
27. Piotto M, Moussallieh FM, Neuville A, Bellocq JP, Elbayed K, Namer IJ. Towards real-time metabolic profiling of a biopsy specimen during a surgical operation by 1H high resolution magic angle spinning nuclear magnetic resonance: a case report. *J Med Case Rep.* 2012;6:22.
28. Cicek AE, Bederman I, Henderson L, Drumm ML, Ozsoyoglu G. ADEMA: an algorithm to determine expected metabolite level alterations using mutual information. *PLoS Comput Biol.* 2013;9:e1002859.
29. Xia J, Bjorndahl TC, Tang P, Wishart DS. MetaboMiner—semi-automated identification of metabolites from 2D NMR spectra of complex biofluids. *BMC Bioinformatics.* 2008;9:507.
30. Lopez-Kolkovsky AL, Mériaux S, Boumezbeur F. Metabolite and macromolecule T1 and T2 relaxation times in the rat brain in vivo at 17.2T. *Magn Reson Med.* 2016;75:503–514.

SUPPORTING INFORMATION

Additional supporting information may be found online in the Supporting Information section at the end of the article.

FIGURE S1 Simplified metabolite pathways used in our laboratory

How to cite this article: Ruhland E, Bund C, Outilaft H, Piotto M, Namer I-J. A metabolic database for biomedical studies of biopsy specimens by high-resolution magic angle spinning nuclear MR: a qualitative and quantitative tool. *Magn Reson Med.* 2019;82:62–83. <https://doi.org/10.1002/mrm.27696>